ITALUS HORTUS
Brief Research Report
Vol. 30 (2023), Pages 70-79
doi: 10.26353/j.itahort/2023.3.7079

Assessing grapevine water status using Sentinel-2 images

Giovanni Caruso and Giacomo Palai*

Department of Agriculture, Food and Environment, University of Pisa
giovanni.caruso@unipi.it
* Corresponding author: giacomo.palai@unipi.it; Tel.: +39-0502616157

Received: 23 October 2023; Accepted: 21 December 2023; Published: 31 December 2023

Abstract: Grapevine water status strongly impacts vine yield and berry quality, hence the importance of a cost- and time-effective methodology to estimate it in commercial vineyards. A two-year experiment was carried out in a rainfed commercial vineyard (cv. 'Vermentino' grafted on '1103P') to test the ability of vegetation indices (VIs) derived from Sentinel-2 (S2) multispectral imagery in estimating the stem water potential (Ψ_{stem}). The S2 VIs calculated including NIR and SWIR bands (NDMI, MSI and NMSI), performed better (R^2 values of 0.66, 0.66 and 0.59, respectively) than those calculated using the bands in the VIS-NIR region (R^2 values 0.47, 0.58 and 0.58 for NDVI, GNDVI and NDWI, respectively). The slope between B8a and B11 bands was also significantly affected by grapevine water status. The different weather conditions occurred during the two experimental years also allowed to observe as the S2 VIs performed better in estimating Ψ_{stem} under prolonged drought conditions. Moreover, S2 VIs were not able to detect differences in grapevine water status during the onset of water stress condition.

Keywords: Remote sensing; Stem water potential; Vegetation indices; *Vitis vinifera* L.

1. Introduction

Water availability is the main environmental factor limiting crop growth and productivity in the Mediterranean region. Dramatic changes in temperature and erratic precipitation patterns will likely make drought events more frequent due to climate change (Guiot et al., 2016). The strong impact of water status on vine productivity and berry quality makes it essential to monitor it carefully to achieve the set yield and quality goals.

Vine water status is commonly quantified by measuring the leaf water potential using the Sholander pressure chamber (Scholander et al., 1965). Predawn leaf water potential (Ψ_{PD}), midday leaf water potential (Ψ_l) and stem water potential (Ψ_{stem}) are the three methods used to assess the plant water status (Choné et al., 2001; Schultz, 1996; Williams et al., 1994). The midday stem water potential is often used to monitor the grapevine water status and it is measured at midday after darkening the leaf for at least one hour in order to balance the water status of the leaf and stem (Choné et al., 2001). Vineyards are normally maintained within a safe Ψ_{stem} range which should not drop below -1.5 MPa, in order to avoid cavitation, turgor loss and leaf shedding (Charrier et al., 2018). In irrigated vineyards, deficit irrigation protocols potentially allow to fine tune the grapevine water stress according to the final farm goals in terms of yield and wine quality (Caruso et al. 2023; Castellarin et al., 2007; Intrigliolo and Castel, 2010). Ψ_{stem} thresholds vary depending on grapevine varieties, phenological stages and oenological objectives (Basile et al., 2011; Girona et al., 2009; Palai et al., 2022). Given the impact of grapevine water status on vineyard performances it is crucial being able to quantify the level of water stress, to identify the vineyard zones most vulnerable to water stress, and to timely determine when water stress occurs. The spatial variability within the vineyard, often induced by soil heterogeneity, further complicates this task. Despite the grapevine water status monitoring can be potentially addressed using the Sholander pressure chamber, the high cost of time and labor of this methodology under high spatial vari-

ability conditions make it poorly suited to this task.

Remote sensing can be an alternative and effective tool to address this issue. Satellite, aircraft and unmanned aerial vehicles (UAVs) are the main platforms used to acquire remote sensing images (Matese et al., 2015). Thermal images acquired from aircraft or drones allow to calculate the crop water stress index (CWSI) which provide information on plant water status, being well correlated with Ψ_{stem} in orchards and vineyards (Baluja et al., 2012; Caruso et al., 2022). Multispectral images from the same platforms have also been used to estimate grapevine water status and identify homogeneous zones within the vineyard for precise irrigation management (Bellvert et al., 2012). The battery capability and the aviation regulation limit the area which UAV can covers, whereas the main critical drawbacks of the aircraft surveys are related to their cost (Matese et al., 2015).

Satellite multispectral images, despite the lower spatial resolution with respect to those acquired from aircraft and UAVs, have been increasingly used for crop monitoring due to their ability to cover large areas and to provide a timely overview of crop conditions. Moreover, the free and open access database of some satellites, such as Sentinel-2 (S2), represents a further important advantage for future farms operational services. Despite the medium-low spatial resolution (10 m to 20 m) of S2 images their spectral [12 bands in the visible (VIS) to Short-Wave Infrared (SWIR) regions] and temporal (5 days revisit time) resolution makes S2 dataset an interesting and versatile tool for crop monitoring (Transon et al., 2018; Weiss et al., 2020).

Previous studies demonstrated that combining the spatial, spectral and temporal resolution of S2 images it is possible to monitor vineyards at large scale highlighting the spatial variability (Di Gennaro et al., 2019). Medium- and low-resolution multispectral images were used to predict grapevine yields (Sun et al., 2017) and leaf area index (LAI) (Anderson et al., 2004; Leolini et al., 2023), and to quantify the impact of heatwaves on the vineyard (Cogato et al. 2019).

The objective of this work was to evaluate whether the VIs retrieved from Sentinel-2 images can be used to estimate grapevine water status in a rainfed vineyard. The effect of the rainfall distribution within the season on the ability of VIs in Ψ_{stem} estimation was also evaluated.

2. Materials and Methods

2.1 Experimental site and plant material

The experiment was carried out during the growing seasons 2022 and 2023 in a 5-year-old rainfed vineyard (*Vitis vinifera* L.) cultivar 'Vermentino' grafted on '1103 Paulsen' (V. *rupestris* x V. *berlandieri*) located in Tuscany (Italy, 43°57 N, 10° 74' E). Vines were planted in a sandy-loam soil at a 0.8 x 2.3 m spacing (NorthEast -SouthWest row orientation) and Guyot pruned and trained with a vertical shoot positioning. The soil was managed at alternate rows maintaining a permanent spontaneous grass or sowing a mixture of cover crops (*Vicia villosa* Roth, *Phacelia tanacetifolia* Benth), x *Triticosecale* Wittmack) after harvest and terminating them with a roller crimper (Clemens GmbH & Co. KG, Wittlich, Germany) at mid-May.

The climatic conditions over the study period were monitored using a weather station iMETOS IMT 300 (Pessl Instruments GmbH, Weiz, Austria) installed on site. Annual precipitation and reference evapotranspiration (ET_0) were 718 and 996 mm in 2022, respectively, and 688 and 1077 mm in 2023. During the summer period (June 21 – September 21), the effective rainfall, calculated as 75% of the daily rainfall, and ET_0 were 96 and 358 mm, in 2022, and 28 and 421 mm in 2023. The average mean air temperature over the same period was 24.3 and 24.2 °C in 2022 and 2023, respectively.

According to the S2 pixels grid, six 20 x 20 m square plots were selected at different positions within the vineyard (Figure 1). Within each plot, three sub-plots were selected on different locations (black dots in Figure 1). In each sub-plot the stem water potential (Ψ_{stem}) was measured on three adjacent vines, for a total of nine Ψ_{stem} measurements per plot (Figure 1). The Ψ_{stem} was measured between 12.00 and 14.00 using a Scholander-type pressure chamber (PMS Instruments, model 600, Albany, OR, USA).

The Ψ_{stem} was measured on one fully expanded leaf per plant inserted near the trunk and covered with aluminum foil for at least 1.5 h before measurements to block leaf transpiration as reported in Caruso et al. (2023).

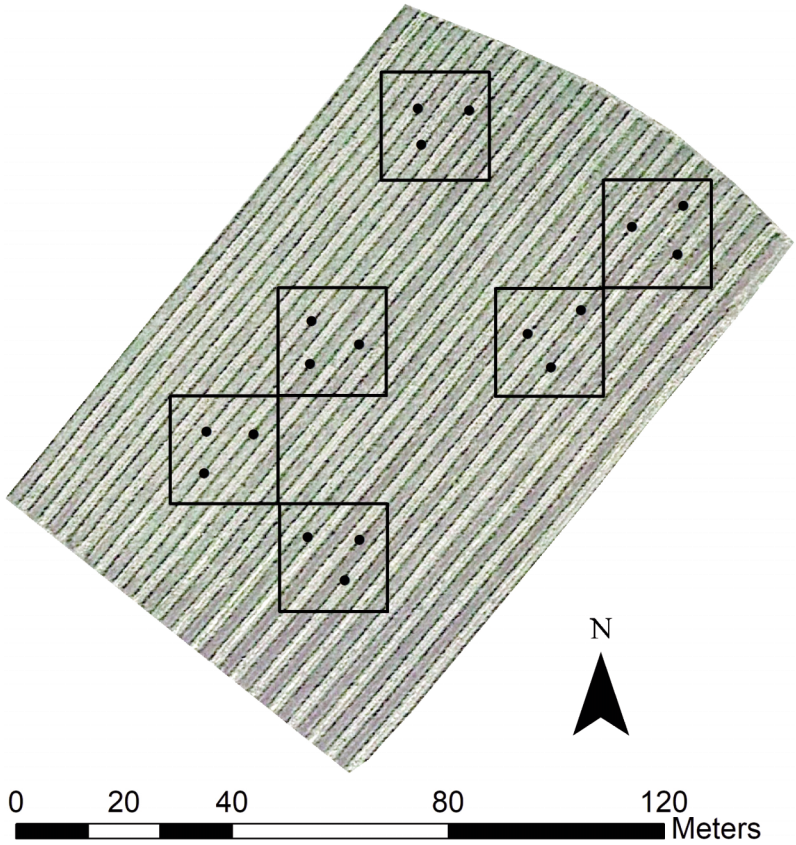

Figure 1. Commercial vineyards used in this study. Black squares represent the six 20 x 20 m plots selected at different positions within the vineyard. Each plot corresponds to the 20 x 20 m S2 pixel. Within each plot, three sub-plots were selected on different locations (black dots) where Ψ_{stem} was measured on three adjacent vines. Image from Google Earth (4 June 2021).

2.2 Satellite Multispectral Imagery and vegetation indices

All the imagery used for this study have been acquired from the constellation of S2 as Level 2A products. Sentinel-2A orthoimages are reflectance calibrated and orthoprojected in WGS84/UTM. A total of ten cloud-free images (five images per year) were downloaded from Copernicus Open Access hub (https://scihub.copernicus.eu/, last access on 15 September 2023) selecting those acquired as close as possible to the dates of Ψ_{stem} measurements (Table 1). The S2 provides images in the visible (VIS), near infrared (NIR) and shortwave infrared (SWIR) range of the electromagnetic spectrum. The central wavelength, the bandwidth and the spatial resolution of the six bands used in this study are reported in Table 2.

Table 1. Date (DOY) of the Ψ_{stem} measurements and of Sentinel-2 images acquisition.

2022		2023	
DOY Ψ_{stem}	DOY Sentinel-2	DOY Ψ_{stem}	DOY Sentinel-2
143	146	162	162
192	197	181	179
210	214	209	205
244	241	229	228
248	248	254	252

Table 2. Spectral bands for the Sentinel-2 sensors considered in this study. Radiometric resolution: 12 bits; Temporal resolution: 5 days. GSD, ground sample distance.

Spectral band	Central wavelength (nm)	Band Width (nm)	GSD (m)
B3 (Green)	560	35	10
B4 (Red)	665	30	10
B8 (Near Infrared)	842	115	10
B8a (Near Infrared Plateau)	885	20	20
B11 (Short wave Infrared 1)	1610	90	20
B12 (Short wave Infrared 2)	2019	180	20

A list of vegetation indices derived from S2 images, and their corresponding formula, are reported in Table 3. The six VIs have been calculated using spectral reflectance ranging from the visible (VIS) to the shortwave infrared (SWIR) bands based on reports from the literature for applications on viticulture (Cohen et al., 2019; Helman et al., 2018).

Table 3. Formulation of the six vegetation indices tested in this study. From Modified Copernicus Sentinel Data-Sentinel Hub (2023). For the calculation of NDMI and MSI the B8a band was used.

Index	Equation
Normalized Difference Vegetation Index (NDVI)	$\frac{B8 - B4}{B8 + B4}$
Green Normalized Difference Vegetation Index (GNDVI)	$\frac{B8 - B3}{B8 + B3}$
Normalized Difference Water Index (NDWI)	$\frac{B3 - B8}{B3 + B8}$
Normalized Difference Moisture Index (NDMI)	$\frac{B8a - B11}{B8a + B11}$
Moisture Index (MSI)	$\frac{B11}{B8a}$
Normalized moisture stress index (NMSI)	$\frac{B8a - B12}{B8a + B12}$

2.3 Data Processing and Statistical Analysis

Ten S2A images were analysed during the study period 2022-2023 (five images per year). For each image the mean values of the different VIs evaluated in this study were calculated for each of the six selected plots, generating a dataset of VIs values time-series for every plot. Image and spatial data processing have been performed with ArcGIS Pro software version 10.3 (Environmental Systems Research Institute, ESRI, Redlands, CA, USA). The statistical relationship between remote sensing data (VIs time-series dataset) and Ψ_{stem} measurements were analyzed by Pearson correlation coefficient using linear relationships in order to estimate which VIs show significant correlation with Ψ_{stem}. Regression analyses were performed using JMP Pro 16.1 (SAS Institute Inc., Drive Cary, NC, USA).

3. Results

The Ψ_{stem} seasonal courses in 2022 and 2023 were clearly affected by the different meteorological conditions over the two experimental years (Figure 2).

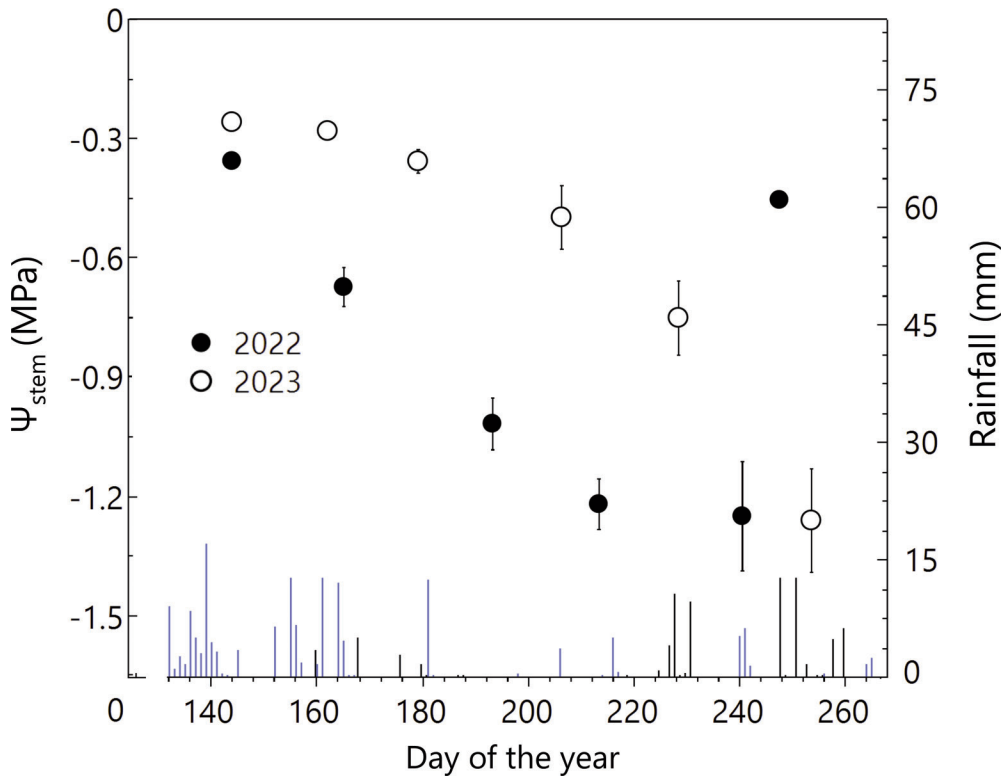

Figure 2. Seasonal course of Ψ_{stem} (dots) and daily rainfall (bars) in 2022 (black dots, black bars) and 2023 (white dots, blue bars, respectively). For Ψ_{stem} each symbol represents the mean ± standard error of 54 Ψ_{stem} measurements.

In particular, 2022 was characterized by a prolonged drought period between May and mid-August, whereas in 2023 the drought period began at mid-June and continued until mid-September, with only four rainfall events accounting for a total of 35 mm. Being the vineyard under rainfed condition the grapevine water status changed during the season accordingly to the precipitation and ET_0. In 2022, Ψ_{stem} showed an early and constant decline from the end of May (DOY 143, -0.33 MPa) until mid-August (DOY 210, -1.04 MPa), when a precipitation event of 40 mm occurred (Figure 2). The Ψ_{stem} remained quite stable until the end of August (DOY 210, -1.07 MPa) and increased to values of non-water stressed vines (-0.41 MPa) on 20 September (DOY 263) after 50 mm precipitation (Figure 2). In 2023 the decrease in Ψ_{stem} started later during the season and was slower than in 2022. Grapevines showed a good water status (Ψ_{stem} of -0.50 MPa) until the end of July (DOY 209). Lower values of Ψ_{stem} were measured on DOY 229 and 254 (Ψ_{stem} of -0.66 and -1.08 MPa, respectively) (Figure 2).

The seasonal courses of NDVI, GNDVI, NDWI, NDMI, MSI and NMSI in 2022 and 2023 are reported in Figure 3. In 2022 a consistency between the time series patterns of the vegetation indices derived from Sentinel-2 and the Ψ_{stem} ones was evident during the entire study period (from DOY146 to DOY 248), whereas in 2023 it was observed only from mid-July to early September (DOY 205 to 252) (Figure 3).

Figure 4 reports the changes in the spectral values of the selected plots during the growing seasons in 2022 and 2023. A general reduction in reflectance values was observed from May to September in both years. Moreover, changes in the ratio between the reflectance values of some individual bands were also observed depending on the grapevine water status. In particular, the slope between B8a and B11 bands changed from negative (Ψ_{stem} above -0.70 MPa) to positive (Ψ_{stem} below -0.90 MPa) values during the season (Figure 2).

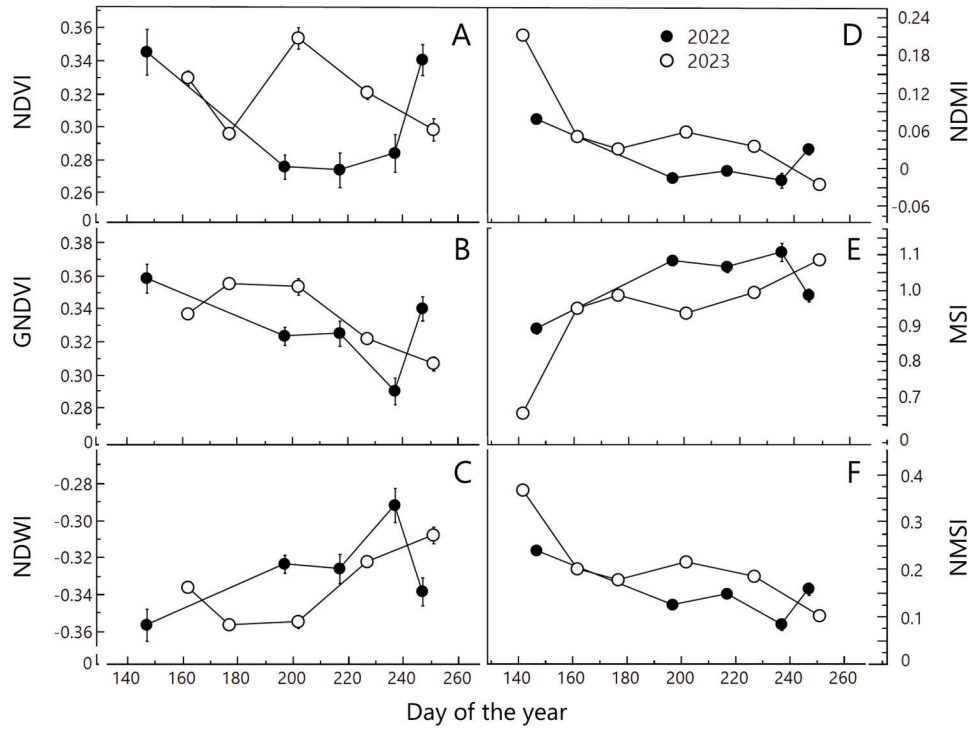

Figure 3. Seasonal course of NDVI, GNDVI, NDWI, NDMI, MSI and NMSI in 2022 (black dots) and 2023 (white dots). Each symbol represents the mean ± standard deviation of the six selected plots.

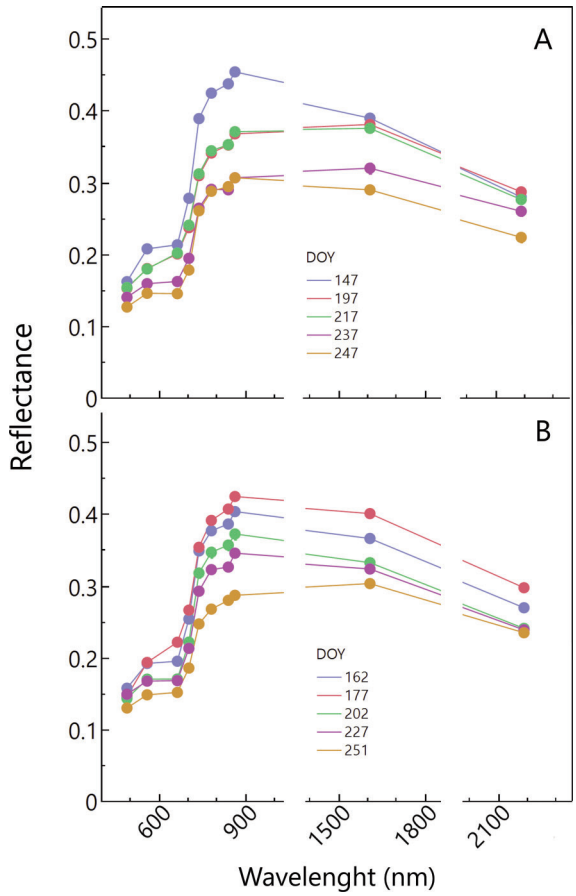

Figure 4. Spectral reflectance values of the selected plots at different dates of image acquisition in 2022 and 2023. Each symbol represents the mean ± standard deviation of six plots.

All the relationships between the S2 derived VIs (NDVI, GNDVI, NDWI, NDMI, MSI and NMSI) and Ψ_{stem} were significant ($p < 0.05$) when both years were plotted together. (Figure 5). The VIs NDMI and MSI showed the strongest relationships with Ψ_{stem} ($R^2 = 0.66$). Among the three VIs including the SWIR bands, the NMSI showed the lowest coefficient of determination values ($R^2 = 0.59$). The VIS-NIR indices showed slightly lower R^2 values (0.47, 0.58 and 0.58 for NDVI, GNDVI and NDWI, respectively). No significant relationships between all the S2 VIs and grapevine water status at Ψ_{stem} values above -0.45 MPa were measured (data not shown).

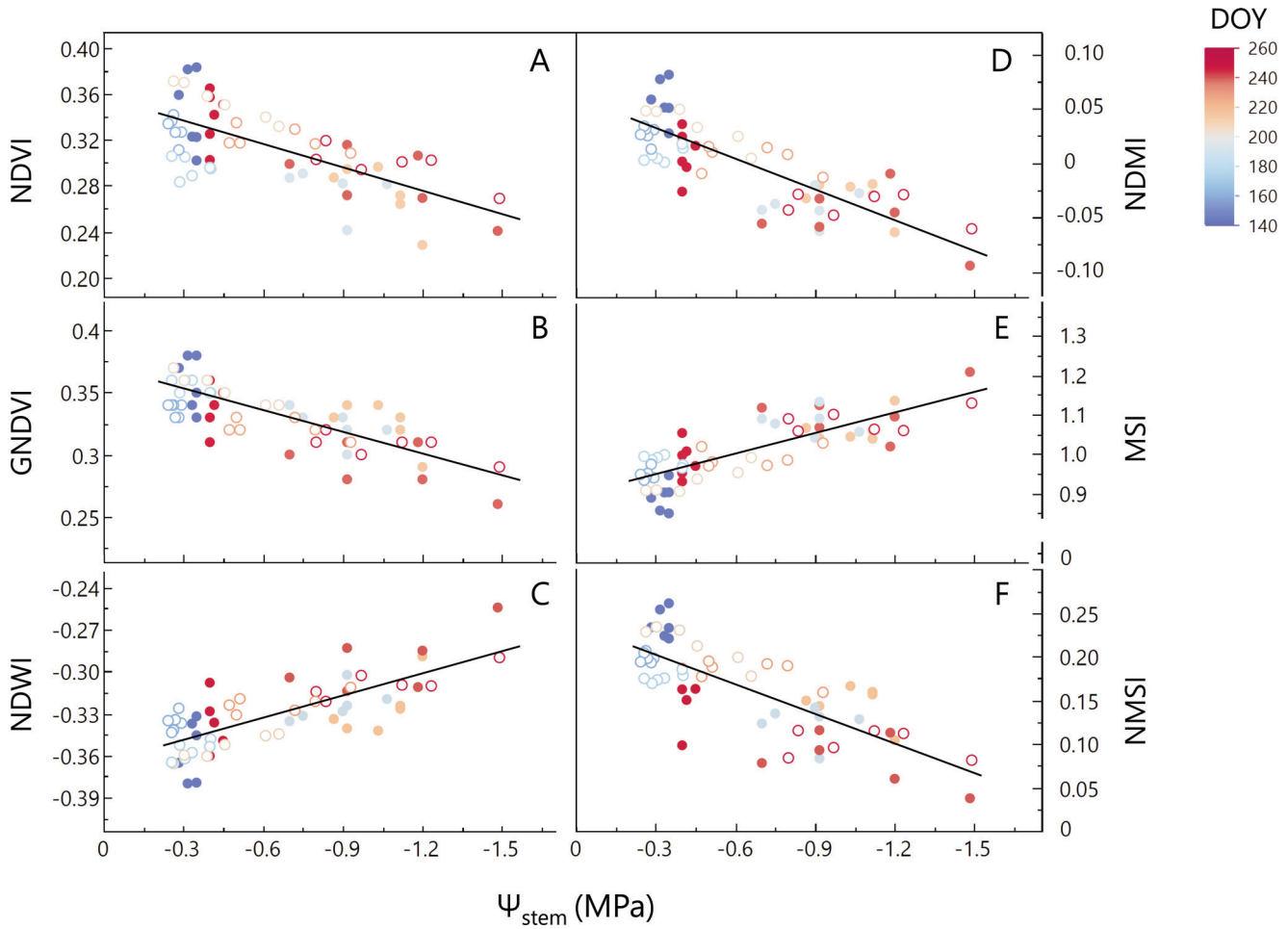

Figure 5. Relationship between the VIs derived from S2 images (NDVI, GNDVI, NDWI, NDMI, MSI and NMSI) and the Ψ_{stem} in 2022 (full symbols) and 2023 (empty symbols). Each symbol represent one experimental plot. Regression equations: A) NDVI = 0.07 Ψ_{stem} + 0.36, $R^2 = 0.47$; B) GNDVI = 0.05 Ψ_{stem} + 0.37, $R^2 = 0.58$; C) NDWI = -0.05 Ψ_{stem} - 0.37, $R^2 = 0.58$; D) NDMI = 0.09 Ψ_{stem} + 0.08, $R^2 = 0.66$; E) MSI = -0.17 Ψ_{stem} + 0.85, $R^2 = 0.66$; F) NMSI = 0.11 Ψ_{stem} + 0.24, $R^2 = 0.59$.

4. Discussion

The climatic conditions over the two experimental years were different between each other and affected the grapevine water status patterns. In 2022 a drought period began in late May and lasted until mid-August. In 2023, grapevines grew under no water limitation until the end of July, then a drought period occurred until the beginning of September. Previous studies have demonstrated the effect of timing, as well as intensity, of water stress on grapevine vegetative growth, yield parameters, and berry quality (Basile et al., 2011; Caruso et al., 2023; Castellarin et al., 2007; Girona et al., 2009; Palai et al., 2022; Palai et al., 2023).

The results of this study allow to derive some considerations on the use of S2 data to estimate the

grapevine water status. First, the S2 VIs calculated including NIR and SWIR bands, in particular NDMI and MSI, performed better than those calculated using the bands in the VIS-NIR region. Similar results have been observed in a previous study carried out in Israel in commercial vineyards where different models using VIS, NIR and SWIR bands were tested for the Ψ_{stem} prediction (Cohen et al., 2019). On the light of these results the indices obtained including the SWIR bands appear to perform better at a commercial level even considering their lower spatial resolution (20 m), with respect to that obtainable using VIS or NIR bands. Second, the S2 VIs were in general not able to detect differences in grapevine water status during the onset of water stress condition. This could explains the general lack of consistency between Ψ_{stem} and VIs patterns in 2023 when the Ψ_{stem} remained above -0.45 MPa until the end of July. On the contrary, the relationships between the VIs tested in this study (NDVI, GNDVI, NDWI, NDMI, MSI and NMSI) and the Ψ_{stem} were more evident at higher level of water stress, highlighting the higher ability in water status monitoring of S2 VIs under medium-high drought conditions. The weak relationship between VIs and Ψ_{stem} under medium-high soil water availability may be attributable to the greater impact of grass cover, in terms of both soil cover and grass vigor, on the S2 images (Palazzi et al., 2023). Therefore, the variability in VIs values observed in 2023 during the period between late spring and early summer may be due to variation in vineyard vigor rather than vineyard water status. An opposite scenario occurred in 2022 when the early and prolonged drought conditions induced a progressive drying out of the grass cover in parallel with an increasing drought condition of the vineyard, with Ψ_{stem} values falling to -0.6 MPa in mid-June and in constant decrease until the end of August. An almost constant decrease of Ψ_{stem} and VIs values derived from high-resolution (3 m) PlanetScope satellite images was also observed in a previous experiment carried out in commercial vineyards located in areas characterized by medium-to-severe water deficit conditions during the entire growing season (Helman et al., 2018).

The impact of the understory vegetation on the mixed pixel spectral response opens to further considerations about the effect of the soil management practices on vineyard monitoring using satellite images. The satisfactory results obtained in this study could be due, at least in part, to the dead mulching technique applied to half of the vineyard floor. This technique, reducing weed growth, allows for a more uniform vegetation understory background. In general, in Mediterranean region, where the grass is usually not very vigorous in summer, or in vineyards where the soil is periodically tilled during the vegetative season, the impact of both soil and understory vegetation background is limited (Pinel et al., 2021). In a previous study carried out in a vineyard without any vegetation cover in the inter-row a strong correlation was found between S2 and UAV-acquired data at both field (R^2= 0.87) and sub-field scale (R^2= 0.84) (Sozzi et al., 2020). Similarly, the different grapevine canopy cover, depending on the developmental stage and/or by the vine vigour, strongly affected the pixel value as observed in previous studies focused on the impact of the grapevine canopy cover on satellite vegetative indices using multispectral images acquired by both UAV and satellites (Leolini et al., 2023; Pinel et al., 2021; Sozzi et al., 2020). Pinel et al. (2021) suggested to determine a threshold of grapevine canopy cover below which the grapevine water status would not be estimated because the insufficient grapevine leaf area would made the derived VIs not representative of the grapevine Ψ_{stem}.

5. Conclusions

The vegetative indices derived from S2 images showed a different ability in estimating Ψ_{stem} depending on the spectral band used for their calculation and on the level of water stress experienced by the monitored vines. The VIs including NIR-SWIR bands performed better than those including only VIS-NIR ones. Significant relationships between VIS and Ψ_{stem} were measured at values below -0.45 MPa, whereas at higher level of soil water availability the vineyard variability was mainly linked to the vineyard vigour than water status. Further investigations are needed to characterize the impact of soil management on S2 VIs performances in grapevine water status estimation.

Funding: This research received no external funding.

Conflicts of Interest: The authors declare no conflict of interest.

References

Anderson M.C., Neale C.M.U., Li F., Norman J.M., Kustas W.P., Jayanthi H. and Chavez J. (2004) 'Upscaling ground observations of vegetation water content, canopy height, and leaf area index during SMEX02 using aircraft and Landsat imagery', *Remote Sensing of Environment*, 92, pp. 447-464. doi: 10.1016/j.rse.2004.03.019

Baluja J., Diago M.P. Balda P., Zorer R., Meggio F., Morales F. and Tardaguila J. (2012) 'Assessment of vineyard water status variability by thermal and multispectral imagery using an unmanned aerial vehicle (UAV)', *Irrigation Science*, 30, pp. 511-522. doi: 10.1007/s00271-012-0382-9

Basile B., Marsal J., Mata M., Vallverdú X., Bellvert J. and Girona J. (2011) 'Phenological sensitivity of Cabernet Sauvignon to water stress: vine physiology and berry composition', *American Journal of Enology and Viticulture*, 62, pp. 452-461. doi: 10.5344/ajev.2011.11003

Bellvert J., Marsal J., Mata M. and Girona J. (2012) 'Identifying irrigation zones across a 7.5-ha 'Pinot noir' vineyard based on the variability of vine water status and multispectral images', *Irrigation Science*, 30(6), pp. 499-509. doi: 10.1007/s00271-012-0380-y

Caruso G., Palai G., Gucci R. and D'Onofrio C. (2023) 'The effect of regulated deficit irrigation on growth, yield, and berry quality of grapevines (cv. Sangiovese) grafted on rootstocks with different resistance to water deficit', *Irrigation Science*, 41, pp. 453-467. doi: 10.1007/s00271-022-00773-3

Caruso G., Palai G., Tozzini L. and Gucci R. (2022) 'Using visible and thermal images by an unmanned aerial vehicle to monitor the plant water status, canopy growth and yield of olive trees (cvs. Frantoio and Leccino) under different irrigation regimes', *Agronomy*, 12, 1904. doi: 10.3390/agronomy12081904

Charrier G., Delzon S., Domec J.C., Zhang L., Delmas C.E.L., Merlin I., Corso D., King A., Ojeda H., Ollat N., Prieto J.A., Scholach T., Skinner P., van Leeuwen C. and Gambetta G.A. (2008) 'Drought will not leave your glass empty: low risk of hydraulic failure revealed by long-term drought observations in world's top wine regions', *Science Advance*, 31, 4. doi: 10.1126/sciadv.aao6969

Castellarin S.D., Matthews M.A., Di Gaspero G. and Gambetta G.A. (2007) 'Water deficits accelerate ripening and induce changes in gene expression regulating flavonoid biosynthesis in grape berries', *Planta*, 227, pp. 101-112. doi: 10.1007/s00425-007-0598-8

Choné X., Van Leeuwen C., Dubourdieu D. and Gaudillères J.P. (2001) 'Stem water potential is a sensitive indicator of grapevine water status', *Annals of Botany*, 87(4), pp. 477-483. doi: 10.1006/anbo.2000.1361

Cogato A., Pagay V., Marinello F., Meggio F., Grace P. and De Antoni Migliorati M. (2019) 'Assessing the feasibility of using Sentinel-2 imagery to quantify the impact of heatwaves on irrigated vineyards' *Remote Sensing*, 11(23), 2869. doi: 10.3390/rs11232869

Cohen Y., Gogumalla P., Bahat I., Netzer Y., Ben-Gal A., Lenski I. and Helman D. (2019) 'Can time series of multispectral satellite images be used to estimate stem water potential in vineyards?' in Stafford J.V. (ed.) *Precision agriculture '19*. The Netherlands: Wageningen Academic Publishers, pp. 445-451. doi: 10.3920/978-90-8686-888-9_55

Di Gennaro S.F., Dainelli R., Palliotti A., Toscano P. and Matese A. (2019) 'Sentinel-2 validation for spatial variability assessment in overhead trellis system viticulture versus UAV and agronomic data', *Remote Sensing*, 11(21), 2573. doi: 10.3390/rs11212573

Girona J., Marsal J., Mata M., Del Campo J. and Basile B. (2009) 'Phenological sensitivity of berry growth and composition of Tempranillo grapevines (Vitis vinifera L.) to water stress', *Australian Journal of Grape and Wine Research*, 15, pp. 268-277. doi: 10.1111/j.1755-0238.2009.00059.x

Guiot J. and Cramer W. (2016) 'Climate change: the 2015 Paris agreement thresholds and mediter-

ranean basin ecosystems', *Science*, 354, pp. 465-468. doi: 10.1126/science.aah5015
Helman D., Bahat I., Netzer Y., Ben-Gal A., Alchanatis V., Peeters A. and Cohen Y. (2018) 'Using time series of high- resolution planet satellite images to monitor grapevine stem water potential in commercial vineyards', *Remote Sensing*, 10, pp. 1615-1637. doi: 10.3390/rs10101615
Intrigliolo D.S. and Castel J.R. (2010) 'Response of grapevine cv. 'Tempranillo' to timing and amount of irrigation: water relations, vine growth, yield and berry and wine composition', *Irrigation Science*, 28, pp. 113-125. doi: 10.1007/s00271-009-0164-1
Leolini L., Bregaglio S., Ginaldi F., Costafreda-Aumedes S., Di Gennaro S.F., Matese A., Maselli F., Caruso G., Palai G., Bajocco S., Bindi M. and Moriondo M. (2023). Use of remote sensing-derived fPAR data in a grapevine simulation model for estimating vine biomass accumulation and yield variability at sub-field level', *Precision Agriculture*, 24, pp. 705-726. doi: 10.1007/s11119-022-09970-8
Matese A., Toscano P., Di Gennaro S.F., Genesio L., Vaccari P., Primicerio J., Belli C., Zaldei A., Bianconi R. and Gioli B. (2015) 'Intercomparison of UAV, aircraft and satellite remote sensing platforms for precision viticulture', *Remote Sensing*, 7, pp. 2971-2990. doi: 10.3390/rs70302971
Modified Copernicus Sentinel data - Sentinel Hub (2023). Available at: https://custom-scripts.sentinel-hub.com/custom-scripts/sentinel/sentinel-2/#remote-sensing-indices (Accessed: October 01, 2023)
Palazzi F., Biddoccu M., Borgogno Mondino E.C. and Cavallo E. (2022) 'Use of remotely sensed data for the evaluation of inter-row cover intensity in vineyards', *Remote Sensing*, 15(1), 41. doi: 10.3390/rs15010041
Pinel E.L., Duthoit S., Costard A.D., Rousseau J., Hourdel J., Vidal-Vigneron M., Cheret V. and Clenet H. (2021) 'Monitoring vineyard water status using Sentinel-2 images: qualitative survey on five wine estates in the south of France', *OENO One*, 55(4), pp. 115-127. doi: 10.20870/oeno-one.2021.55.4.4752
Palai G., Caruso G., Gucci R. and D'Onofrio C. (2022) 'Berry flavonoids are differently modulated by timing and intensities of water deficit in Vitis vinifera L. cv. Sangiovese', *Frontiers in Plant Science*, 13, 1040899. doi: 10.3389/fpls.2022.1040899
Palai G., Caruso G., Gucci R. and D'Onofrio C. (2023) 'Water deficit before veraison is crucial in regulating berry VOCs concentration in Sangiovese grapevines', *Frontiers in Plant Science*, 14:1117572. doi: 10.3389/fpls.2023.1117572
Scholander P.F., Bradstreet E.D., Hemmingsen E.A. and Hammel H.T. (1965) 'Sap pressure in vascular plants: negative hydrostatic pressure can be measured in plants', *Science*, 148(3668), pp. 339-346. doi: 10.1126/science.148.3668.339
Sozzi M., Kayad A., Marinello F., Taylor J.A. and Tisseyre B. (2020) 'Comparing vineyard imagery acquired from Sentinel-2 and unmanned aerial vehicle (UAV) platform', *Oeno One*, 54(2), pp.189–197. doi: 10.20870/oeno-one.2020.54.1.2557
Sun L., Gao F., Anderson M.C., Kustas W.P., Alsina M.M., Sanchez L., Sams B., McKee L., Dulaney W., White W.A., Alfieri J.G., Prueger J.H., Melton F. and Post K. (2017) 'Daily mapping of 30 m LAI and NDVI for grape yield prediction in California vineyards', *Remote Sensing*, 9, 317. doi: 10.3390/rs9040317
Transon J., D'Andrimont R., Maugnard A. and Defourny P. (2018) 'Survey of hyperspectral Earth Observation applications from space in the Sentinel-2 context', *Remote Sensing*, 10, 157. doi: 10.1109/Multi-Temp.2017.8035244
Weiss M., Jacob F. and Duveiller G. (2020) 'Remote sensing for agricultural applications: A meta-review', *Remote Sensing of Environment*, 236, 111402. doi: 10.1016/j.rse.2019.111402

© 2023 by the authors. Licensee Italian Society for Horticultural Science (Società di Ortoflorofrutticoltura Italiana; SOI), Sesto Fiorentino (Firenze), Italy. This work is an open access article distributed under a Creative Commons Attribution-NonCommercial (CC BY NC) 4.0 International License (http://creativecommons.org/licenses/by-nc/4.0/).